PERGAMON

International Journal of Solids and Structures 36 (1999) 2303–2319

INTERNATIONAL JOURNAL OF SOLIDS and STRUCTURES

Finite element analysis of the piezoelectric vibrations of quartz plate resonators with higher-order plate theory

Ji Wang[a,]*, Yook-Kong Yong[b], Tsutomu Imai[c]

[a]*Epson Palo Alto Laboratory, 3145 Porter Drive, Suite 104, Palo Alto, CA 94304, U.S.A.*
[b]*Department of Civil and Environmental Engineering, Rutgers University, Piscataway, NJ 08855, U.S.A.*
[c]*Quartz Crystal Device Laboratory, Seiko Epson Corporation, 3-3-5 Owa, Suwa-shi, Nagano-ken 392, Japan*

Received 29 September 1997; in revised form 12 March 1998

Abstract

A finite element formulation of the piezoelectric vibrations of quartz resonators based on Mindlin plate theory is derived. The higher-order plate theory is employed for the development of a collection of successively higher-order plate elements which can be effective for a broad frequency range including the fundamental and overtone modes of thickness-shear vibrations. The presence of electrodes is also considered for their mechanical effects.

The mechanical displacements and electric potential are combined into a generalized displacement field, and the subsequent derivations are carried out with all the generalized equations. Through the standard finite element procedure, the vibration frequency, the vibration mode shapes and the electric potential distribution are obtained. The frequency spectra are compared with some well-known experimental results with good agreement.

Our previous experience with finite element analysis of high-frequency quartz plate vibrations leads us to believe that memory and computing time will always remain as key issues despite the advances in computers. Hence, the use of sparse matrix techniques, efficient eigenvalue solvers, and other reduction procedures are explored.

1. Introduction

The application of finite element method in the analysis of vibrations of quartz crystal plate resonators has been studied by many authors in the last decades, and practical results have been obtained gradually through these efforts. Given the fact that the problem is greatly complicated by the higher vibration frequency, which means fundamental thickness-shear frequency here, in

* Corresponding author. Tel.: 001 650 843 8336. Fax: 001 650 843 9106. E-mail: jiwang@epal.com

PII: S0020–7683(98)00108–5

comparison with the conventional structural vibration problem in flexural modes and limited interest in the finite element analysis, only a few of the programs developed so far have found applications in the design process and analysis of new products, but further interest have been inspired by the increasingly active research projects and promising results which could have a big impact on the design of quartz crystal resonators in the future.

Even though the analytical approach of plate resonators has been restricted to the two-dimensional plate equations with straight-crested wave solutions (see e.g. Mindlin and Gazis, 1962; Lee and Wang, 1994; Wang and Momosaki, 1997) for obvious reasons, the finite element formulations have been drawn from three-dimensional piezoelectricity equations and various two-dimensional plate theories. Lee and Tang (1986) implemented the finite element analysis of the first-order Mindlin plate equations for the stress sensitivity and vibration analysis of circular crystal resonators. With the three-dimensional incremental theory for frequency-temperature relations of quartz crystals, Yong (1987) studied the frequency-temperature behavior of crystal bar, plate, and tuning-fork type resonators. Later, the two-dimensional incremental theory were implemented for the finite element analysis of plate resonators (Yong, 1988). Canfield et al. (1991, 1992) studied the same problem with the implementation of the three-dimensional piezoelectricity with thermal effect considerations. Mindlin first-order plate theory was implemented for the mechanical vibrations of crystal resonators by Yong et al. (1991, 1992) and for the frequency shift due to temperature variations by Antonova and Silvester (1994). In the finite element implementation of Lee plate theory, Yong and Zhang (1993, 1994) developed a perturbation technique to consider the piezoelectric effect in the modeling of quartz plate resonators. The same finite element program was also used for straight-crested wave solutions of thin film piezoelectric resonators by Zhang and Yong (1995). To reduce the number of equations in the two-dimensional finite element implementation of the plate theory, a creative one-dimensional finite element formulation has been crafted by Sekimoto and Watanabe (1990). Noting that the higher-order plate theory may actually reduce the number of equations in the finite element implementation in comparison with three-dimensional approach (Zhang and Yong, 1995), which is particularly important in the high frequency vibration analysis, Yong et al. (1996) implemented Mindlin higher-order plate theory for quartz resonator analysis with finite strip formulation. Of course, the systematic study of the accuracy of plate theories by Yong et al. (1996) is the basis of the applications of higher-order theories. Mindlin third-order plate theory is also used for the finite element study of the frequency-temperature behavior of crystal resonators by Yong (1996). Lerch (1990) and Lerch and Bauereschmidt (1996) extended the application of the piezoelectric three- and two-dimensional finite element program into the analysis of quartz resonators. By approximating the electric field, Stewart and Stevens (1997) employed the three-dimensional finite element method for the crystal resonator analysis. The computing techniques and resources available for finite element analysis, including efficient and reliable eigenvalue solvers, sparse matrix handling techniques, and parallel computing have been explored and utilized (Jones and Plassmann, 1992; Yong and Cho, 1996). Applications of general purpose finite element software such as ANSYS have also been reported by several authors (see e.g. Momosaki and Kogure, 1982; Beeby and Tudor, 1995; Söderkvist, 1997; Gehin et al., 1997).

In this study, we start with Mindlin higher-order plate theory for piezoelectric crystal plates. In the finite element formulation, we define the components of the mechanical displacements and electric potential as the generalized displacement, and as a consequence the generalized stress and

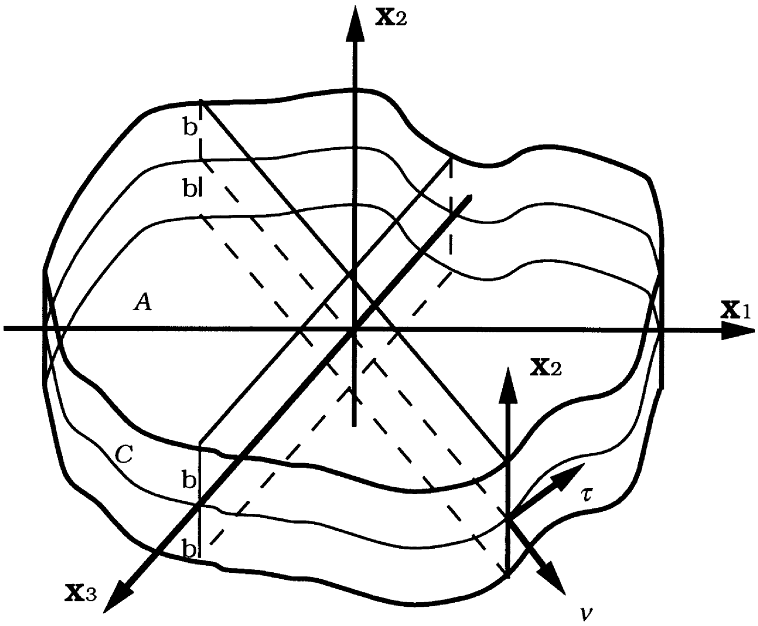

Fig. 1. Plate coordinates and boundaries.

strain are also defined in a similar manner. Eventually, this results in a generalized implementation which is very close to the conventional one for mechanical vibration analysis except the mass terms corresponding to the electric potential are zeroes, which leads to a more sparser mass matrix. The sparse matrix handling techniques are employed in the assembling and solving of the eigenvalue problems. Finally, we compare the numerical results of the vibration spectrum of a crystal plate to the well-known experimental measurements by Koga (1963), and excellent agreement has been observed.

2. Fundamentals of mindlin plate theory

The fundamental equations of Mindlin higher-order piezoelectric plate theory (Mindlin, 1972, 1984) are based on the infinite power series expansion of the mechanical displacements and electric potential in thickness coordinate x_2, as shown in Fig. 1, to

$$u_j(x_1, x_2, x_3, t) = \sum_{n=0} u_j^{(n)}(x_1, x_3, t)x_2^n,$$

$$\phi(x_1, x_2, x_3, t) = \sum_{n=0} \phi^{(n)}(x_1, x_3, t)x_2^n, \tag{1}$$

where $u_j^{(n)}$ and $\phi^{(n)}$ are nth-order two-dimensional components of the displacements and potential.

The strain–mechanical displacement and electric field–electric potential relations of the higher-order plate theory can be written as

$$S_{ij}^{(n)} = \tfrac{1}{2}[u_{i,j}^{(n)} + u_{j,i}^{(n)} + (n+1)(\delta_{i2}u_j^{(n+1)} + \delta_{j2}u_i^{(n+1)})],$$
$$E_i^{(n)} = -\phi_{,i}^{(n)} - (n+1)\delta_{i2}\phi^{(n+1)}, \tag{2}$$

where δ_{i2} is the Kronecker delta.

The two-dimensional linear piezoelectric constitutive equations are

$$T_{ij}^{(n)} = \sum_{m=0} B_{mn}(c_{ijkl}S_{kl}^{(m)} - e_{kij}E_k^{(m)}),$$
$$D_i^{(n)} = \sum_{m=0} B_{mn}(e_{ijk}S_{jk}^{(m)} + \varepsilon_{ij}E_j^{(m)}), \tag{3}$$

where $T_{ij}^{(n)}$, $D_i^{(n)}$, $S_{kl}^{(m)}$, $E_k^{(m)}$, c_{ijkl}, e_{kij}, and ε_{ij} are stress components, electric displacement components, strain components, electric field components, elastic constants, piezoelectric constants, and dielectric constants, respectively. The integral constant B_{mn} is

$$B_{mn} = \begin{cases} \dfrac{2b^{m+n+1}}{m+n+1}, & m+n = \text{even}, \\ 0, & m+n = \text{odd}. \end{cases} \tag{4}$$

The two-dimensional stress equations of motion and electrostatics derived from the three-dimensional ones are

$$T_{ij,i}^{(n)} - nT_{2j}^{(n-1)} + B_{nn}T_j^{(n)} = \rho \sum_{m=0} B_{mn}\ddot{u}_j^{(m)},$$
$$D_{i,i}^{(n)} - nD_2^{(n-1)} + B_{nn}D^{(n)} = 0, \tag{5}$$

with

$$T_j^{(n)} = \frac{1}{B_{nn}} b^n[T_{2j}(b) - (-1)^n T_{2j}(-b)],$$
$$D^{(n)} = \frac{1}{B_{nn}} b^n[D_2(b) - (-1)^n D_2(-b)], \tag{6}$$

where ρ, $T_j^{(n)}$, $D^{(n)}$, $T_{2j}(b)$, $T_{2j}(-b)$, $D_2(b)$, and $D_2(-b)$ are the density of the crystal, face traction difference, face charge difference, upper face traction, lower face traction, upper face charge, and lower face charge, respectively.

The boundary conditions for the two-dimensional equations can be directly derived from the three-dimensional ones with the known expansions of the displacements and potential in power series. By defining the nth-order surface traction and charge as

$$t_j^{(n)} = \frac{1}{B_{nn}} \int_{-b}^{b} t_j x_2^n \, \mathrm{d}x_2, \quad \sigma^{(n)} = \frac{1}{B_{nn}} \int_{-b}^{b} \sigma x_2^n \, \mathrm{d}x_2, \tag{7}$$

where t_j and σ are prescribed surface traction and charge, we have the following natural boundary conditions

$$t_j = T_{2j}, \quad \sigma = D_2 \quad \text{on } A, \quad j = 1,2,3,$$
$$t_j^{(n)} = n_a T_{aj}^{(n)}, \quad \sigma^{(n)} = n_a D_a^{(n)} \quad \text{on } C, \quad a = 1,3, \tag{8}$$

or their alternatives

$$u_j = \bar{u}_j, \quad \phi = \bar{\phi} \quad \text{on } A,$$
$$u_j^{(n)} = \bar{u}_j^{(n)}, \quad \phi^{(n)} = \bar{\phi}^{(n)} \quad \text{on } C, \tag{9}$$

where the barred quantities represent the prescribed boundary values on A and C. It should be noted that the boundary conditions in eqn $(8)_1$ are already incorporated into eqn (5) by specifying $T_j^{(n)}$ and $D^{(n)}$ according to eqn (6).

These equations have been extensively used for the straight-crested wave solutions of crystal resonators in conjunction with some approximate techniques such as truncation and one-dimensional approximation (see e.g. Lee and Wang, 1994; Wang and Momosaki, 1997). By formulating and implementing the higher-order equations in a systematic manner, we hope that a finite element program can be developed for the vibration analysis of crystal resonators at not only the fundamental thickness-shear but also the higher-order overtone frequencies.

3. Modifications of the plate equations

The higher-order plate equations given in the previous section are complete for the vibration analysis of quartz plates, and their application is straightforward. However, given the fact that in piezoelectric resonators the crystal plates are always electroded, modifications are needed for both the mechanical and piezoelectric vibration analyses. Furthermore, we need a proper procedure to reduce the infinite system and correct and compensate the finite set of equations for practical and accurate solutions. These modifications, as have been made before by many authors, include the consideration of the mechanical effects of the platings of the electrodes, the corrections of the truncated plate equations, and the truncation procedure itself. These procedures have been developed and employed for many years, and they can be treated as the standard procedures for the applications of higher-order plate theories. Through the modifications we present below, the plate theory introduced before will be tailored for the crystal resonator vibration analysis at the fundamental thickness-shear and overtone frequencies.

3.1. The mechanical effects of platings

The thin layers of metal platings on crystal plates for thickness excitation purpose are usually treated as mass loading on the crystal plates, and it has been studied by Mindlin (1963), Tiersten (1969) and Lee et al. (1987).

We assume the thickness of the platings on both sides of the crystal are identical and denoted them as $2b'$, and the density of the platings is ρ'. The tractions on the faces of the plated crystal are

$$T_{2j}(b) = T_{2j}(B) - 2b'\rho'\ddot{u}_j(b),$$

$$T_{2j}(-b) = T_{2j}(-B)+2b'\rho'\ddot{u}_j(-b), \tag{10}$$

where $B = b+2b'$, and $T_{2j}(B)$ and $T_{2j}(-B)$ are the face tractions on the platings.

By substituting eqn (10) into eqn $(6)_1$, the difference of the crystal face tractions will be

$$\begin{aligned} T_j^{(n)} &= \frac{1}{B_{nn}}[b^n T_{2j}(b)-(-b)^n T_{2j}(-b)] \\ &= \mathscr{T}_j^{(n)} - \frac{b^n}{B_{nn}} 2b'\rho'[\ddot{u}_j(b)+(-1)^n \ddot{u}_j(-b)], \end{aligned} \tag{11}$$

where $\mathscr{T}_j^{(n)}$ is the difference of the face tractions of the platings.

In each mode for long wavelengths, we have

$$u_j(b) = \sum_{n=0} b^n u_j^{(n)}, \quad u_j(-b) = \sum_{n=0} (-b)^n u_j^{(n)}, \tag{12}$$

hence eqn (11) is further simplified to

$$\begin{aligned} B_{nn} T_j^{(n)} &= B_{nn}\mathscr{T}_j^{(n)} - 2b'\rho' 2b^{2n} \ddot{u}_j^{(n)} \\ &= B_{nn}\mathscr{T}_j^{(n)} - \rho \sum_{m=0} (m+n+1) R B_{mn} \ddot{u}_j^{(n)}, \end{aligned} \tag{13}$$

where

$$R = \frac{2b'\rho'}{b\rho}, \tag{14}$$

is the mass ratio of the electrodes to the crystal.

Now the stress equations of motion in eqn (5) with platings will be modified to

$$T_{ij,i}^{(n)} - nT_{2j}^{(n-1)} + B_{nn}\mathscr{T}_j^{(n)} = \rho \sum_{m=0} B_{mn}[1+(m+n+1)R]\ddot{u}_j^{(m)}. \tag{15}$$

The mechanical effects in eqn (15) are consistent with similar equations by others (Mindlin, 1963; Tiersten, 1965).

3.2. Truncations of the equations

The two-dimensional infinite system has to be truncated to a finite set for their solutions, and a standard truncation procedure proposed by Mindlin (1955, 1972, 1984) has been widely employed (Lee and Wang, 1994). In this study we demonstrate the procedure for the truncation of the third-order theory of AT-cut quartz plates by setting

$$\begin{aligned} & u_1^{(n)} = u_3^{(n)} = \phi^{(n)} = T_p^{(n)} = D_i^{(n)} = 0 \quad \text{for } n > 3, \\ & T_2^{(3)} = 0, \quad u_2^{(4)} \neq 0, \quad \dot{u}_2^{(4)} = 0, \quad u_2^{(n)} = 0 \quad \text{for } n > 4, \\ & p = 1,2,3,4,5,6, \quad i = 1,2,3, \end{aligned} \tag{16}$$

and from eqn $(3)_1$ we have

$$c_{22}4u_2^{(4)} = -\frac{7}{5b^2}[c_{21}u_{1,1}^{(1)} + c_{22}2u_2^{(2)} + c_{23}u_{3,3}^{(1)} + c_{24}(u_{2,3}^{(1)} + 2u_3^{(2)})] + c_{21}u_{1,1}^{(3)} + c_{23}u_{3,3}^{(3)} + c_{24}u_{2,3}^{(3)}$$

$$+\frac{7}{5b^2}(e_{12}E_1^{(1)} + e_{22}E_2^{(1)} + e_{32}E_3^{(1)}) + e_{12}E_1^{(3)} + e_{22}E_2^{(3)} + e_{32}E_3^{(3)}. \quad (17)$$

With the given $u_2^{(4)}$ in eqn (17), we can update all the equations containing $S_2^{(3)}$, which are stress component $T_p^{(1)}$ and $T_p^{(3)}$ $(p = 1,2,3,4,5,6)$ and electric displacement component $D_i^{(1)}$ and $D_i^{(3)}$ $(i = 1,2,3)$, to

$$\begin{aligned}
T_p^{(1)} &= B_{11}\tilde{c}_{pq}S_q^{(1)} + B_{31}\bar{c}_{pq}S_q^{(3)} - B_{11}\tilde{e}_{kp}E_k^{(1)} - B_{31}\bar{e}_{kp}E_k^{(3)},\\
T_p^{(3)} &= B_{13}\bar{c}_{pq}S_q^{(1)} + B_{33}\bar{c}_{pq}S_q^{(3)} - B_{13}\bar{e}_{kp}E_k^{(1)} - B_{33}\bar{e}_{kp}E_k^{(3)},\\
D_i^{(1)} &= B_{11}\tilde{e}_{iq}S_q^{(1)} + B_{31}\bar{e}_{iq}S_q^{(3)} + B_{11}\tilde{\varepsilon}_{ik}E_k^{(1)} + B_{31}\bar{\varepsilon}_{ik}E_k^{(3)},\\
D_i^{(3)} &= B_{13}\tilde{e}_{iq}S_q^{(1)} + B_{33}\bar{e}_{iq}S_q^{(3)} + B_{13}\tilde{\varepsilon}_{ik}E_k^{(1)} + B_{33}\bar{\varepsilon}_{ik}E_k^{(3)},
\end{aligned} \quad (18)$$

with

$$\begin{aligned}
\bar{c}_{pq} &= c_{pq} - \frac{c_{p2}c_{2q}}{c_{22}}, \quad \tilde{c}_{pq} = c_{pq} - \frac{21}{25}\frac{c_{p2}c_{2q}}{c_{22}},\\
\bar{e}_{kp} &= c_{kp} - \frac{c_{p2}e_{k2}}{c_{22}}, \quad \tilde{e}_{kp} = c_{kp} - \frac{21}{25}\frac{c_{p2}e_{k2}}{c_{22}},\\
\bar{\varepsilon}_{ik} &= \varepsilon_{ik} + \frac{e_{i2}e_{k2}}{c_{22}}, \quad \tilde{\varepsilon}_{ik} = \varepsilon_{ik} + \frac{21}{25}\frac{e_{i2}e_{k2}}{c_{22}},\\
p,q &= 1,2,3,4,5,6, \quad i,k = 1,2,3.
\end{aligned} \quad (19)$$

Truncations for higher-order equations and other cuts can be carried out in a similar fashion. In the finite element implementation, we have truncated the equations upto the fifth-order. It has also been observed from our computation that the truncations and the resulted modifications to the material constants have significant effect on certain branches of the frequency spectra.

3.3. Correction factors

The truncation of the first-order equations requires correction factors to warrant accurate results, and many correction factors have been suggested (see e.g. Mindlin, 1955, 1963, 1972; Tiersten, 1969) with various considerations including the presence of electrodes. In this study, the correction factors proposed by Mindlin (1955) is used as

$$\bar{c}_{pq} = \kappa_p\kappa_q c_{pq}, \quad \bar{e}_{ip} = \kappa_p e_{ip}, \quad \kappa_p = \begin{cases} \frac{\pi^2}{12}, & p,q = 2,4,6,\\ 1, & p,q = 1,3,5. \end{cases} \quad (20)$$

These truncated and corrected equations with plating considerations will be the plate equations for finite element implementation. In the computer program, the plate theory upto the fifth-order is implemented so the computation can be made in a wide frequency range. The selection of the order of the plate theory for the computation has been discussed by Yong et al. (1995), but we also find that the aspect ratios and the frequency are the important factors.

4. Variational principles

The two-dimensional variational equations of higher-order plate theory, which will be the basis of the finite element formulation, for mechanical vibrations can be given as (see e.g. Mindlin, 1955, 1972, 1984; Tiersten, 1969)

$$\sum_n \int_A \left(T_{ij,i}^{(n)} - nT_{2j}^{(n-1)} + B_{nn} T_j^{(n)} - \rho \sum_{m=0} B_{mn} \ddot{u}_j^{(m)} \right) \delta u_j^{(n)} \, \mathrm{d}A = 0. \tag{21}$$

By applying the divergence theorem, we have

$$\begin{aligned} \int_A T_{ij,i}^{(n)} \delta u_j^{(n)} \, \mathrm{d}A &= \int_A [(T_{ij}^{(n)} \delta u_j^{(n)})_{,i} - T_{ij}^{(n)} \delta u_{j,i}^{(n)}] \, \mathrm{d}A \\ &= \int_C f_j^{(n)} \delta u_j^{(n)} \, \mathrm{d}S - \int_A T_{ij}^{(n)} \delta u_{j,i}^{(n)} \, \mathrm{d}A, \end{aligned} \tag{22}$$

where n_i is the outward surface normal of the boundary, and the surface traction $f_j^{(n)}$ is defined as

$$f_j^{(n)} = n_i T_{ij}^{(n)}. \tag{23}$$

By definition we have

$$\sum_n (T_{ij}^{(n)} \delta u_{j,i}^{(n)} + nT_{2j}^{(n-1)} \delta u_j^{(n)}) = \sum_n T_{ij}^{(n)} \delta S_{ij}^{(n)}. \tag{24}$$

The substitution of eqns (22) and (24) into eqn (21) yields the variational equations of mechanical vibrations as

$$\sum_n \int_A \left(T_{ij}^{(n)} \delta S_{ij}^{(n)} + \rho \sum_{m=0} B_{mn} \ddot{u}_j^{(m)} \delta u_j^{(n)} \right) \mathrm{d}A = \sum_n \left(\int_C f_j^{(n)} \delta u_j^{(n)} \, \mathrm{d}S + \int_A F_j^{(n)} \delta u_j^{(n)} \, \mathrm{d}A \right), \tag{25}$$

where

$$F_j^{(n)} = B_{nn} T_j^{(n)}. \tag{26}$$

In a similar fashion, we have variational equations of electrostatics as

$$\sum_n \int_A D_i^{(n)} \delta E_i^{(n)} \, \mathrm{d}A = -\sum_n \left(\int_C q^{(n)} \delta \phi^{(n)} \, \mathrm{d}S + \int_A Q^{(n)} \delta \phi^{(n)} \, \mathrm{d}A \right), \tag{27}$$

and the surface charges and face charges are defined as

$$q^{(n)} = n_i D_i^{(n)}, \quad Q^{(n)} = B_{mn} D^{(n)}. \tag{28}$$

For a piezoelectric solid we have the virtual electric enthalpy density definition (Mindlin, 1972)

$$\delta W = T_{ij}^{(n)} \delta S_{ij}^{(n)} - D_i^{(n)} \delta E_i^{(n)}, \tag{29}$$

thus the previous variational eqns (25) and (27) can be combined into

$$\sum_n \int_A \left[(T_{ij}^{(n)} \delta S_{ij}^{(n)} - D_i^{(n)} \delta E_i^{(n)})\, \mathrm{d}A + \rho \sum_{m=0} B_{mn} \ddot{u}_j^{(m)} \delta u_j^{(n)}\, \mathrm{d}A \right] = \sum_n \int_C (f_j^{(n)} \delta u_j^{(n)} + q^{(n)} \delta \phi^{(n)})\, \mathrm{d}S + \sum_n \int_A (F_j^{(n)} \delta u_j^{(n)} + Q^{(n)} \delta \phi^{(n)})\, \mathrm{d}A. \tag{30}$$

Now we can use the variational eqn (30) for the finite element formulation of the higher-order plate theory. Ostensibly, the combination of the two variational equations, as we shall show next, is intended to aid the generalized formulation of the piezoelectric plate vibration problem.

5. Generalized finite element formulation

Traditionally, piezoelectric problems have been formulated by separating the mechanical variables, which are displacements, and electric variables, which are electric potentials in most cases, in the formation of the linear equation systems (see e.g. Allik and Hughes, 1970; Lerch, 1990; Yong and Zhang, 1993, 1994, 1995). By taking this approach, the two sets of equations will be eventually reduced to the mechanical vibration problem through the elimination of the electric one, and many techniques have been proposed for the condensation of the stiffness matrix (Allik and Hughes, 1970; Lerch, 1990), including a perturbation technique (Yong and Zhang, 1993, 1994, 1995). However, it has also been noticed lately that the generalized approach, which means the mechanical displacement and electric potentials will be combined to form a generalized displacement field, may also be advantageous since the costly condensation of the stiffness matrix can be avoided to speed up the eigenvalue computation (Yong and Cho, 1996).

In this paper, the higher-order piezoelectric plate theory is presented in a generalized matrix form to facilitate the finite element implementation. The representative matrices are illustrated, again, with the third-order plate theory.

We start with the generalized nth-order displacement field $u_j^{(n)}$ ($n = 0, 1, 2, 3$)

$$\mathbf{u}^{(n)} = \{u_1^{(n)}, u_2^{(n)}, u_3^{(n)}, \phi^{(n)}\}_{4 \times 1}, \tag{31}$$

and accordingly we have the generalized displacement vector from the third-order plate theory as

$$\mathbf{u} = \{\mathbf{u}^{(0)}, \mathbf{u}^{(1)}, \mathbf{u}^{(2)}, \mathbf{u}^{(3)}\}_{16 \times 1}. \tag{32}$$

We further define the generalized nth-order strain and stress vectors as

$$\mathbf{S}^{(n)} = \{S_1^{(n)}, S_2^{(n)}, S_3^{(n)}, S_4^{(n)}, S_5^{(n)}, S_6^{(n)}, E_1^{(n)}, E_2^{(n)}, E_3^{(n)}\}_{9 \times 1},$$
$$\mathbf{T}^{(n)} = \{T_1^{(n)}, T_2^{(n)}, T_3^{(n)}, T_4^{(n)}, T_5^{(n)}, T_6^{(n)}, D_1^{(n)}, D_2^{(n)}, D_3^{(n)}\}_{9 \times 1}. \tag{33}$$

From the generalized strain–displacement relations in eqn (2), by rearranging the terms, we can write

$$\mathbf{S}^{(n)} = \partial_u \mathbf{u}^{(n)} + \partial_u^{(n+1)} \mathbf{u}^{(n+1)}, \tag{34}$$

where the two strain operators are defined as

$$\partial_u = \begin{bmatrix} \frac{\partial}{\partial x_1} & 0 & 0 & 0 \\ 0 & 0 & 0 & 0 \\ 0 & 0 & \frac{\partial}{\partial x_3} & 0 \\ 0 & \frac{\partial}{\partial x_3} & 0 & 0 \\ \frac{\partial}{\partial x_3} & 0 & \frac{\partial}{\partial x_1} & 0 \\ 0 & \frac{\partial}{\partial x_1} & 0 & 0 \\ 0 & 0 & 0 & -\frac{\partial}{\partial x_1} \\ 0 & 0 & 0 & 0 \\ 0 & 0 & 0 & -\frac{\partial}{\partial x_3} \end{bmatrix}_{9\times 4},$$

$$\partial_u^{(n+1)} = (n+1) \begin{bmatrix} 0 & 0 & 0 & 0 \\ 0 & 1 & 0 & 0 \\ 0 & 0 & 0 & 0 \\ 0 & 0 & 1 & 0 \\ 0 & 0 & 0 & 0 \\ 1 & 0 & 0 & 0 \\ 0 & 0 & 0 & 0 \\ 0 & 0 & 0 & -1 \\ 0 & 0 & 0 & 0 \end{bmatrix}_{9\times 4}, \tag{35}$$

and finally, eqn (34), we define the generalized strain vector, with

$$\mathbf{S} = \begin{Bmatrix} \mathbf{S}^{(0)} \\ \mathbf{S}^{(1)} \\ \mathbf{S}^{(2)} \\ \mathbf{S}^{(3)} \end{Bmatrix}_{36\times 1} = \partial_S \mathbf{u}$$

$$= \begin{bmatrix} \partial_u & \partial_u^{(1)} & \mathbf{0} & \mathbf{0} \\ \mathbf{0} & \partial_u & \partial_u^{(2)} & \mathbf{0} \\ \mathbf{0} & \mathbf{0} & \partial_u & \partial_u^{(3)} \\ \mathbf{0} & \mathbf{0} & \mathbf{0} & \partial_u \end{bmatrix}_{36\times 16} \begin{Bmatrix} \mathbf{u}^{(0)} \\ \mathbf{u}^{(1)} \\ \mathbf{u}^{(2)} \\ \mathbf{u}^{(3)} \end{Bmatrix}_{16\times 1}. \tag{36}$$

The linear piezoelectric constitutive relations given in eqn (3) can also be generalized and written in matrix form as

$$\mathbf{T} = \mathbf{CS}, \tag{37}$$

where

$$\mathbf{C} = \begin{bmatrix} B_{00}\bar{\mathbf{C}} & \mathbf{0} & B_{02}\bar{\mathbf{C}} & \mathbf{0} \\ \mathbf{0} & B_{11}\bar{\mathbf{C}} & \mathbf{0} & B_{13}\bar{\mathbf{C}} \\ B_{20}\bar{\mathbf{C}} & \mathbf{0} & B_{22}\bar{\mathbf{C}} & \mathbf{0} \\ \mathbf{0} & B_{31}\bar{\mathbf{C}} & \mathbf{0} & B_{33}\bar{\mathbf{C}} \end{bmatrix}_{36\times 36},$$

$$\bar{\mathbf{C}} = \begin{bmatrix} \mathbf{c} & -\mathbf{e}^T \\ \mathbf{e} & \varepsilon \end{bmatrix}_{9\times 9}. \tag{38}$$

It is interesting to note that the generalized material constant matrix is no longer symmetric.

In matrix form, the variational eqn (30) can be written as

$$\int_A (\delta\mathbf{S}^T\mathbf{cS} - \delta\mathbf{S}^T\mathbf{e}^T\mathbf{E} - \delta\mathbf{E}^T\mathbf{eS} - \delta\mathbf{E}^T\varepsilon\mathbf{E} + \rho\delta\mathbf{u}^T\mathbf{m}\ddot{\mathbf{u}})\,\mathrm{d}A = \int_C (\delta\mathbf{u}^T\mathbf{f} + \delta\phi^T\mathbf{q})\,\mathrm{d}S + \int_A (\delta\mathbf{u}^T\mathbf{F} + \delta\phi^T\mathbf{Q})\,\mathrm{d}A, \tag{39}$$

where **m**, **f**, **q**, **F**, and **Q** are the mass matrix, the surface traction vector, surface charge vector, face traction vector, and face charge vector, respectively, are to be combined into the generalized surface traction and face traction from now on.

In generalized notations we can write eqn (39) as

$$\int_A \delta\mathbf{S}^T\mathbf{DS}\,\mathrm{d}A + \int_A \rho\delta\mathbf{u}^T\mathbf{m}\ddot{\mathbf{u}}\,\mathrm{d}A = \int_C \delta\mathbf{u}^T\mathbf{f}\,\mathrm{d}S + \int_A \delta\mathbf{u}^T\mathbf{F}\,\mathrm{d}A, \tag{40}$$

where

$$\mathbf{D} = \begin{bmatrix} B_{00}\bar{\mathbf{D}} & \mathbf{0} & B_{02}\bar{\mathbf{D}} & \mathbf{0} \\ \mathbf{0} & B_{11}\bar{\mathbf{D}} & \mathbf{0} & B_{13}\bar{\mathbf{D}} \\ B_{20}\bar{\mathbf{D}} & \mathbf{0} & B_{22}\bar{\mathbf{D}} & \mathbf{0} \\ \mathbf{0} & B_{31}\bar{\mathbf{D}} & \mathbf{0} & B_{33}\bar{\mathbf{D}} \end{bmatrix}_{36\times 36},$$

$$\bar{\mathbf{D}} = \begin{bmatrix} \mathbf{c} & -\mathbf{e}^T \\ -\mathbf{e} & -\varepsilon \end{bmatrix}_{9\times 9},$$

$$\mathbf{m} = \begin{bmatrix} \mathbf{m}_0^{(0)} & \mathbf{0} & \mathbf{m}_0^{(2)} & \mathbf{0} \\ \mathbf{0} & \mathbf{m}_1^{(1)} & \mathbf{0} & \mathbf{m}_1^{(3)} \\ \mathbf{m}_2^{(0)} & \mathbf{0} & \mathbf{m}_2^{(2)} & \mathbf{0} \\ \mathbf{0} & \mathbf{m}_3^{(1)} & \mathbf{0} & \mathbf{m}_3^{(3)} \end{bmatrix}_{16\times 16},$$

$$\mathbf{m}_m^{(n)} = \rho B_{mn}[1+(m+n+1)R] \begin{bmatrix} 1 & 0 & 0 & 0 \\ 0 & 1 & 0 & 0 \\ 0 & 0 & 1 & 0 \\ 0 & 0 & 0 & 0 \end{bmatrix}_{4\times 4}. \tag{41}$$

It should be emphasized that the mass matrix has zero terms corresponding to the electric potentials.

Following the conventional discretization procedure, we start the finite element implementation with

$$\mathbf{u} = \begin{bmatrix} \mathbf{u}^{(0)} \\ \mathbf{u}^{(1)} \\ \mathbf{u}^{(2)} \\ \mathbf{u}^{(3)} \end{bmatrix}_{16\times 1} = [\hat{\mathbf{N}}_1 \hat{\mathbf{N}}_2, \ldots, \hat{\mathbf{N}}_l]_{16\times 16l} \begin{bmatrix} \mathbf{U}_1 \\ \mathbf{U}_2 \\ \vdots \\ \mathbf{U}_l \end{bmatrix}_{16l\times 1} = \mathbf{NU},$$

$$\hat{\mathbf{N}}_i = N_i \mathbf{I}_{16\times 16}, \quad \mathbf{S} = \partial_S \mathbf{NU} = \mathbf{BU},$$

$$\mathbf{B} = [\mathbf{B}_1 \mathbf{B}_2, \ldots, \mathbf{B}_l], \quad i = 1, 2, \ldots, l, \tag{42}$$

where l is the number of nodes of each element, $\mathbf{U}$ is the discretized displacement vector, N_i are the shape functions, $\mathbf{I}$ is the identity matrix, and the $\mathbf{B}_i$ matrix is given as

$$\mathbf{B}_i = \begin{bmatrix} \partial_u N_i & \partial_u^{(1)} N_i & \mathbf{0} & \mathbf{0} \\ \mathbf{0} & \partial_u N_i & \partial_u^{(2)} N_i & \mathbf{0} \\ \mathbf{0} & \mathbf{0} & \partial_u N_i & \partial_u^{(3)} N_i \\ \mathbf{0} & \mathbf{0} & \mathbf{0} & \partial_u N_i \end{bmatrix}_{36\times 16}. \tag{43}$$

The discretization of the variational eqn (40) gives

$$\delta \mathbf{U}^T \left(\int_A \mathbf{B}^T \mathbf{DB}\, \mathrm{d}A \mathbf{U} + \int_A \mathbf{N}^T \mathbf{mN}\, \mathrm{d}A \ddot{\mathbf{U}} - \int_C \mathbf{N}^T \mathbf{f}\, \mathrm{d}S - \int_A \mathbf{N}^T \mathbf{F}\, \mathrm{d}A \right) = 0, \tag{44}$$

and the discretized and generalized equations of motion in matrix form as

$$\mathbf{KU} + \mathbf{M}\ddot{\mathbf{U}} = \mathbf{F}_C + \mathbf{F}_A, \tag{45}$$

where

$$\mathbf{K} = \int_A \mathbf{B}^T\mathbf{D}\mathbf{B}\,\mathrm{d}A, \quad \mathbf{M} = \int_A \mathbf{N}^T\mathbf{m}\mathbf{N}\,\mathrm{d}A,$$

$$\mathbf{F}_C = \int_C \mathbf{N}^T\mathbf{f}\,\mathrm{d}S, \quad \mathbf{F}_A = \int_A \mathbf{N}^T\mathbf{F}\,\mathrm{d}A, \tag{46}$$

are generalized stiffness matrix, mass matrix, surface traction vector, and face traction vector, respectively.

Now we have the conventional finite element equation given in eqn (45), which is the identical one we already know in structural mechanics problems, where the finite element method has been intensively studied for decades. By adopting this formulation, it is hoped that all the sophisticated techniques can be utilized.

For free vibrations, by setting the traction vectors to zero and assuming the solution is harmonic, we have the generalized vibration eigenvalue problem from eqn (45)

$$\mathbf{KU} - \omega^2\mathbf{MU} = 0, \tag{47}$$

where ω is the vibration frequency. Usually we normalized the frequency by the fundamental thickness-shear frequency

$$\omega_0 = \frac{\pi}{2b}\sqrt{\frac{c_{66}}{\rho}}. \tag{48}$$

It is clear from the matrix equations that the mass matrix is no longer diagonal due to the coupling of modes, and the off-diagonal terms have to be included in the computations. A comparison with the conventional finite element analysis will tell that this will add further difficulty to the eigenvalue computation. The high vibration frequency will also require a finer mesh, which translates to a very large, usually several millions, linear equation system. For this reason, an efficient eigenvalue solver can handle sparse matrix computation, which is standard in most finite element analysis programs today, is essential to this program. Also it should be realized that we have a critical requirement for such eigenvalue solvers, namely they should be able to extract all the eigenvalues inside a given frequency interval, usually in the vicinity of the resonance vibration frequency. Eigenvalue solvers capable of this kind of computation are difficult to find, and extra efforts have to be made to modify the existing ones in public domains such as the Netlib, or locate available commercial codes.

As an example, we computed the frequency spectra of a crystal plate with third-order plate theory and four-node element to make comparisons with the experimental data by Koga (1963). It is found that the frequency spectra from pure mechanical vibrations agree well with the measurement in Fig. 2, and the frequency change due to piezoelectric effect is clearly displayed in Fig. 3. The frequency difference between mechanical and piezoelectric vibrations is shown in Fig. 4.

6. Conclusions

The higher-order Mindlin plate theory has been systematically modified for applications in the piezoelectric vibration analysis of crystal resonators for the resonance frequency spectrum. By

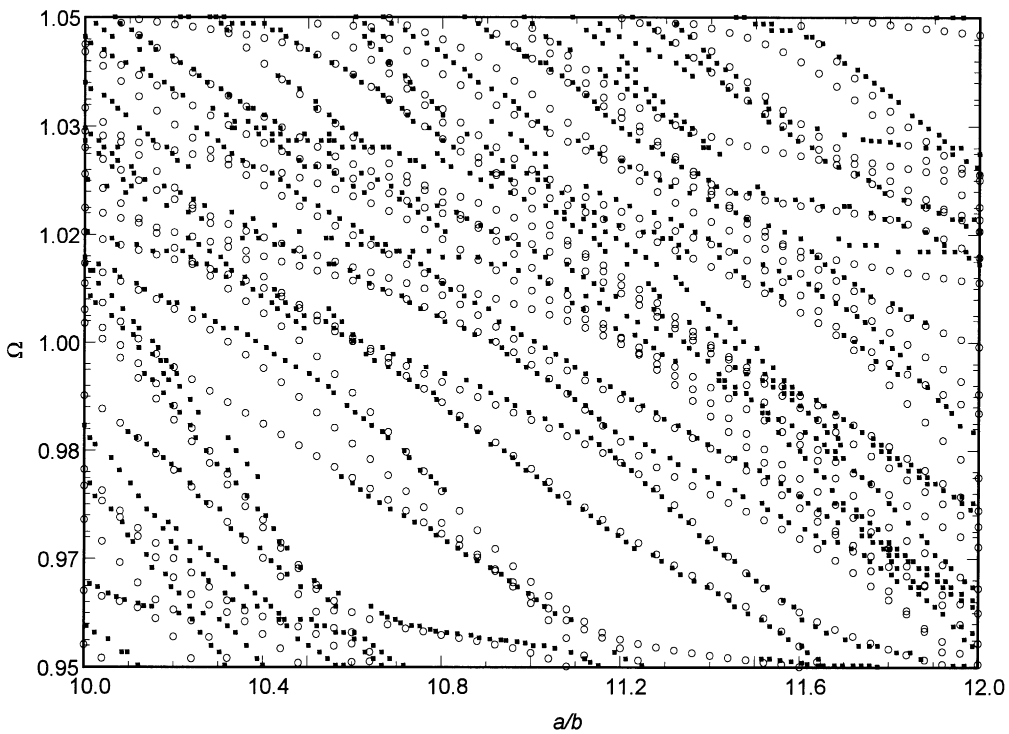

Fig. 2. Normalized frequency vs length to thickness ratio for a crystal plate with width to thickness ratio $c/b = 16.3660$. The computed frequency spectra from the mechanical vibrations (○) is compared with the experimental data (dark square) from Koga (1963).

adopting a generalized approach, the modified plate theory is successfully implemented for the finite element solutions for the vibration problems which have been extensively studied but never been able to solve for the precise and accurate modeling of crystal resonators. From the comparisons of the numerical results of the mechanical and piezoelectric vibrations, we found that this generalized formulation is straightforward and effective for the piezoelectric plate vibration problems. The results also confirmed the long time view widely known to researchers that the piezoelectric effects on the free vibrations of the crystal plates can be neglected in the frequency spectrum analysis since the frequency shift is tiny and uniform. For practical purposes, the frequency spectrum from the mechanical vibrations will provide a valuable and precise pattern for better selection of plate geometry. We also found that we have produced the frequency spectra from both the mechanical and piezoelectric vibrations which match the experimental data well.

It is agreed that the modeling of piezoelectric devices with finite element method continues to be a challenge, partially due to the extremely high frequency, which requires the unusually larger number of equations, in comparison with conventional finite element analysis applications. This challenge spreads further to strict requirement for efficient mathematical subroutines essential to the analysis, namely the eigenvalue solvers and linear equation solvers. Fortunately, the mathematical community has been inspired and encouraged by these rigorous attempts, and tremendous progress

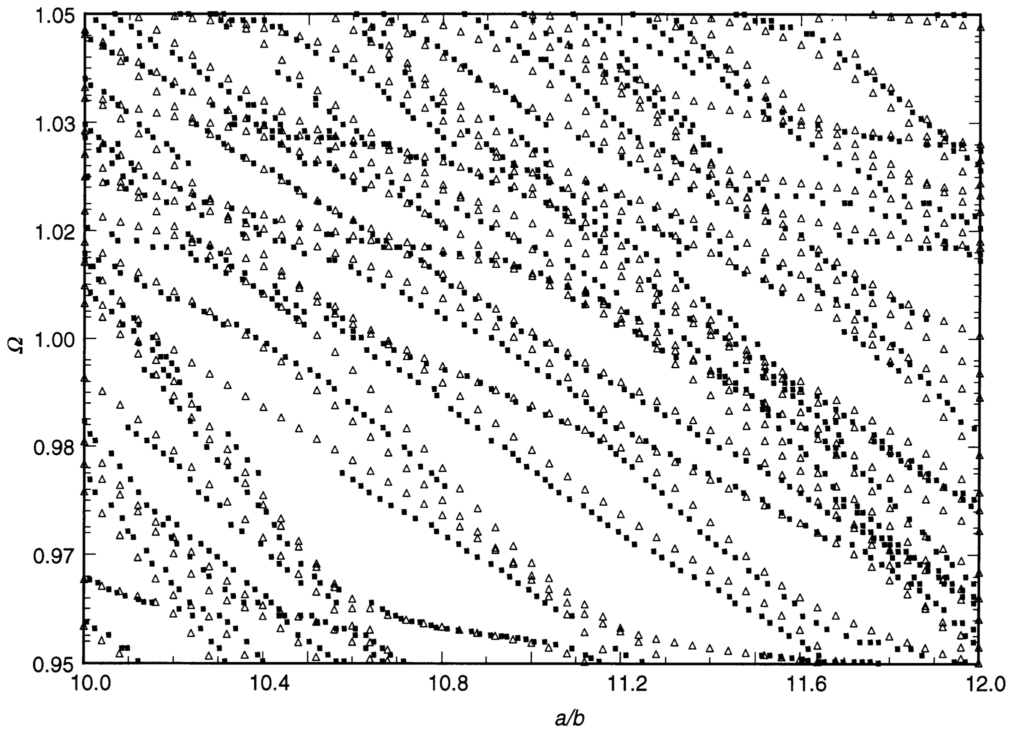

Fig. 3. Normalized frequency vs length to thickness ratio for a crystal plate with width to thickness ratio $c/b = 16.3660$. The computed frequency spectra from the piezoelectric vibrations (△) is compared with the experimental data (dark square) from Koga (1963).

has been made for the efficient and fast solvers, while such efforts are continuing to meet the demands for even larger problems. Also the availability of powerful computers provides another opportunity, particularly with the proliferation of multiple processors systems which can be easily programmed to solve the larger number of equations from the problem.

On the piezoelectricity theory, tremendous efforts have been made to make the approximate theories to be able to solve the real problem easily and accurately. These efforts will also assist the better finite element implementation for less equations but accurate results. Particularly, the efforts in reducing the order of the plate theory and the elimination of the electric variable from the equations will have great impact on the computing aspect.

With the combination of the efforts in all directions, it is expected that we shall be able to provide efficient and accurate numerical solutions to assist the crystal resonator development.

Acknowledgements

The first author thanks Mr Roger Grimes of Boeing for helpful discussions in the eigenvalue computing and Dr Akio Ishizaki and Professor Yasuaki Watanabe of Tokyo Metropolitan University for the experimental data.

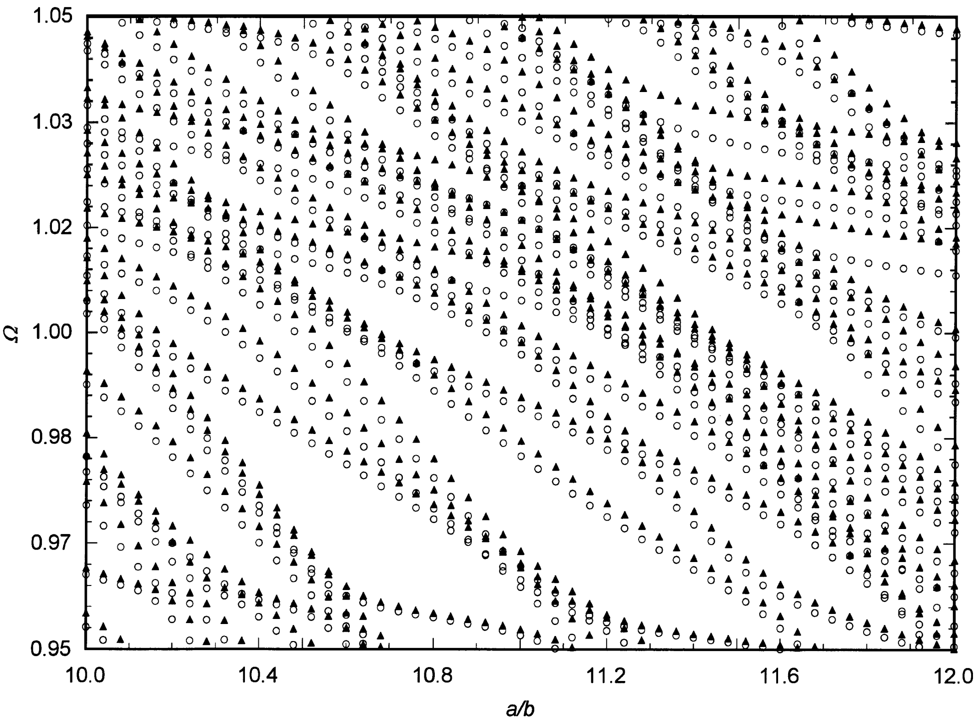

Fig. 4. Comparison of the computed normalized frequency vs length to thickness ratio from the piezoelectric vibrations (△) and mechanical vibrations (○) for a crystal plate with width to thickness ratio $c/b = 16.3660$.

References

Allik, H. and Hughes, T. J. R. (1970) Finite element method for piezoelectric vibration. *Int. J. Numer. Methods Eng.* **2,** 151–157.

Antonova, E. E. and Silvester, P. P. (1994) Finite element analysis of resonance shift in piezoelectric crystals. *The International Journal for Computation and Mathematics in Electrical and Electronic Engineering* **13** (Supplement A), 277–282.

Beeby, S. P. and Tudor, M. J. (1995) Modeling and optimization of micromachined silicon resonators. *J. Micromech. Microeng.* **5,** 103–105.

Canfield, T. R., Jones, M. T., Plassmann, P. E. and Tang, M. S. H. (1992) Thermal effects on the frequency response of piezoelectric crystals. *Proceedings of the* 1992 *Pressure Vessels and Piping Conference* **246,** 103–107.

Canfield, T. R., Tang, M. S. H. and Foster, J. E. (1991) *Non-linear Geometric and Thermal Effects in Three Dimensional Galerkin Finite-element Formulations for Piezoelectric Crystals.* Technical Report, Computing and Telecommunication Division, Argonne National Laboratory, Argonne, IL 60439.

Gehin, C., Samper, S. and Teisseyre, Y. (1997) Mounting characterization of piezoelectric resonator using FEM. *Proceedings of* 1997 *International IEEE Frequency Control Symposium*, pp. 630–633.

Jones, M. T. and Plassmann, P. E. (1992) Solution of large, sparse systems of linear equations in massively parallel applications. *Proceedings of Supercomputing '*92, pp. 551–560. IEEE Computer Society Press.

Koga, I. (1963) Radio-frequency vibrations of rectangular *AT*-cut quartz plates. *Journal of Applied Physics* **34**(8), 2357–2365.

Lee, P. C. Y., Syngellakis, S. and Hou, J. P. (1987) A two-dimensional theory for high-frequency vibrations of piezoelectric crystal plates with or without electrodes. *Journal of Applied Physics* **61**(4), 1249–1262.

Lee, P. C. Y. and Tang, M. S. H. (1986) Initial stress field and resonance frequencies of incremental vibrations in crystal resonators by finite element method. *Proceedings of the* 40*th Annual Frequency Control Symposium*, pp. 152–160.

Lee, P. C. Y. and Wang, J. (1994) Vibrations of *AT*-cut quartz strips of narrow width and finite length. *Journal of Applied Physics* **75**(12), 7681–7695.

Lerch, R. (1990) Simulation of piezoelectric devices by two- and three-dimensional finite elements. IEEE Trans. Ultrason., Ferroelec., Freq. Contr., **37**(2), 233–247.

Lerch, R. and Bauerschmidt, P. (1996) Optical voltage sensor based on a quartz resonator. *Proceedings of the* 1996 *IEEE Ultrasonics Symposium*, pp. 383–387.

Mindlin, R. D. (1955) *An Introduction to the Mathematical Theory of Vibrations of Elastic Plates*. U.S. Army Signal Corps Engineering Laboratories, Fort Monmouth, NJ.

Mindlin, R. D. (1963) High frequency vibrations of plated, crystal plates. *Progress in Applied Mechanics*, pp. 73–84. Macmillan, New York.

Mindlin, R. D. (1972) High frequency vibrations of piezoelectric crystal plates. *International Journal of Solids and Structures* **8,** 895–906.

Mindlin, R. D. (1984) Frequencies of piezoelectrically forced vibrations of electroded, doubly rotated, quartz plates. *International Journal of Solids and Structures* **20**(2), 141–157.

Mindlin, R. D. and Gazis, D. C. (1962) Strong resonance of rectangular *AT*-cut quartz plates. *Proceedings of the* 4*th U.S. National Congress in Applied Mechanics*, pp. 305–310.

Momosaki, E. and Kogure, S. (1982) The application of piezoelectricity to watches. *Ferroelectrics* **40,** 203–216.

Sekimoto, H. and Watanabe, Y. (1990) Two-dimensional analysis of thickness-shear and flexural vibrations in rectangular *AT*-cut quartz plates using a one-dimensional finite element method. *Proceedings of the* 44*th Annual Symposium on Frequency Control*, pp. 358–362.

Söderkvist, J. (1997) Using FEA to treat piezoelectric low-frequency resonators. *Proceedings of* 1997 *IEEE International Frequency Control Symposium*, pp. 634–642.

Stewart, J. T. and Stevens, D. S. (1997) Three dimensional finite element modeling of quartz crystal strip resonators. *Proceedings of* 1997 *IEEE International Frequency Control Symposium*, pp. 643–649.

Tiersten, H. F. (1969) *Linear Piezoelectric Plate Vibrations*. Plenum Press, New York.

Wang, J. and Momosaki, E. (1997) The piezoelectrically forced vibrations of *AT*-cut quartz strip resonators. *Journal of Applied Physics* **81**(4), 1868–1876.

Yong, Y.-K. (1987) Three-dimensional finite-element solution of the Lagrangian equations for the frequency-temperature behavior of *Y*-cut and *NT*-cut bars. *IEEE Trans. Ultrason., Ferroelec., Freq. Contr.* **34**(5), 491–499.

Yong, Y.-K. (1988) Characteristics of a Lagrangian, high-frequency plate element for the static temperature behavior of low-frequency quartz resonator. *IEEE Trans. Ultrason., Ferroelec., Freq. Contr.* **35**(6), 788–799.

Yong, Y.-K. (1996) Third-order Mindlin plate theory predictions for the frequency-temperature behavior of straightened crested wave modes in *AT*- and *SC*-cut quartz plates. *Proceedings of the* 1996 *IEEE International Frequency Control Symposium*, pp. 648–656.

Yong, Y.-K. and Cho, Y. (1996) Numerical algorithms for solutions of large eigenvalue problems in piezoelectric resonators. *Int. J. Numer. Methods Eng.* **39,** 909–922.

Yong, Y.-K. and Stewart, J. T. (1991) Mass-frequency influence surface mode shapes, and frequency spectrum of a rectangular *AT*-cut quartz plate. *IEEE Trans. Ultrason., Ferroelec., Freq. Contr.* **38**(1), 67–73.

Yong, Y.-K., Stewart, J. T., Detaint, J., Zarka, A., Capelle, B. and Zheng, Y. (1993) Thickness-shear mode shapes and mass-frequency influence surface of a circular and electroded *AT*-cut quartz resonators. *IEEE Trans. Ultrason., Ferroelec., Freq. Contr.* **39**(5), 609–617.

Yong, Y.-K., Wang, J., Imai, T., Kanna, S. and Momosaki, E. (1996) A set of hierarchical finite elements for quartz plate resonators. *Proceedings of the* 1996 *IEEE Ultrasonics Symposium*, pp. 981–985.

Yong, Y.-K. and Zhang, Z. (1993) A perturbation method for finite element modeling of piezoelectric vibrations in quartz plate resonators. *IEEE Trans. Ultrason., Ferroelec., Freq. Contr.* **40**(5), 551–562.

Yong, Y.-K. and Zhang, Z. (1994) Numerical algorithms and results for *SC*-cut quartz plates vibrating at the third harmonic overtone of thickness shear. *IEEE Trans. Ultrason., Ferroelec., Freq. Contr.* **41**(5), 685–693.

Yong, Y.-K. and Zhang, Z. and Hou, J. (1996) On the accuracy of plate theories for the prediction of unwanted modes near the fundamental thickness-shear mode. *IEEE Trans. Ultrason., Ferroelec., Freq. Contr.* **43**(5), 888–892.

Zhang, Z. and Yong, Y.-K. (1995) Numerical analysis of thickness shear thin film piezoelectric resonators using a laminated plate theory. *IEEE Trans. Ultrason., Ferroelec., Freq. Contr.* **42**(4), 734–746.